JOURNAL OF CATALYSIS 95, 57–70 (1985)

# Direct Measurements of Heats of Adsorption on Platinum Catalysts

## I. $H_2$ on Pt Dispersed on $SiO_2$, $Al_2O_3$, $SiO_2$–$Al_2O_3$, and $TiO_2$

M. ALBERT VANNICE, LORI C. HASSELBRING, AND BISHWAJIT SEN

*Department of Chemical Engineering, The Pennsylvania State University, University Park, Pennsylvania 16802*

Received March 8, 1985; revised April 9, 1985

Isothermal, integral heats of adsorption have been measured for $H_2$ adsorption on Pt dispersed on four supports. These values were determined at 215 and 300–320 K using a modified differential scanning calorimeter. At room temperature $\Delta H_{(ad)}$ ranged from 21 to 36 kcal/mole on the "typical" Pt catalysts, which included $Pt/TiO_2$ (low-temperature reduction, LTR) reduced at 473 K. The heats of adsorption were highest on $Pt/SiO_2$ and lowest on $Pt/TiO_2$ (LTR); however, a clear trend exists between $\Delta H_{(ad)}$ and Pt fraction exposed, with large Pt crystallites having the highest values. A high-temperature reduction (HTR) at 773 K of $Pt/TiO_2$ markedly decreased both chemisorption and the heat of adsorption, with values as low as 5–10 kcal/mole occurring after repeated HTR cycles. These results provide direct evidence that a decrease in the H–Pt bond strength can be at least partially responsible for lower chemisorption capacity; however, migration of $TiO_x$ species onto the Pt is assumed to cause physical blockage of some Pt sites as well as modification of the chemical properties of the few remaining *surface* Pt atoms that are available for adsorption. A linear correlation exists between the logrithm of the $CH_4$ turnover frequency and the $H_2$ heat of adsorption. 

## INTRODUCTION

Since the report by Tauster *et al.* that high-temperature reduction (HTR) near 773 K markedly decreased the $H_2$ and CO chemisorption capacity of Group VIII metals dispersed on $TiO_2$ (*1*), many studies have been directed toward a better understanding of this phenomenon. A number of explanations for this behavior currently exist, one of which is the proposal that bond strengths between the adsorbate and the metal are decreased as a consequence of an electronic effect caused by some form of electron transfer between the metal and the support (*2–4*). Another explanation, which does not require a decrease in heats of adsorption, is that chemisorption is decreased because of physical blockage of metal surface sites created by the migration of the support onto the metal surface (*5–7*).

One principal goal in this study was the direct calorimetric measurement of heats of adsorption of CO and $H_2$ on Pt dispersed on $TiO_2$ along with those obtained for "typical" Pt catalysts utilizing $SiO_2$, $Al_2O_3$, and $SiO_2$–$Al_2O_3$ as supports. A comparison of these results should help determine whether a decreased heat of adsorption for CO and $H_2$ is the primary cause for lower chemisorption uptakes. It was also of interest to measure these isothermal, integral heats of adsorption because these values relate to surfaces equilibrated at high gas pressures which can exist under reaction conditions. Another reason for this investigation was the large variation in methanation turnover frequency which has been found for this family of catalysts (*8*), and the correlation which has been observed between heats of adsorption and activity (*9*). It was therefore of interest to determine whether any relationship between these two parameters existed for these Pt catalysts. This initial paper describes the differential scanning calorimetry (DSC) system and its modifications in detail and discusses $H_2$ adsorption, while CO adsorption is dis-



0021-9517/85 $3.00

cussed in the second paper in this series (*10*).

## EXPERIMENTAL

### *Catalyst Preparation*

The catalysts used in this study were prepared from chloroplatinic acid and $\eta$-$Al_2O_3$ (Exxon Research & Engineering Co.), $SiO_2$–$Al_2O_3$ (Davison Grade 979, 13% alumina), $TiO_2$ (P-25 from Degussa Co., 80% anatase and 20% rutile), and $SiO_2$ (Davidson Grade 57). The reported surface areas for each support are 245, 400, 50, and 220 $m^2\ g^{-1}$, respectively. The 2.1% Pt/$\eta Al_2O_3$, 1.5% Pt/$TiO_2$, 2.0% Pt/$TiO_2$ and 2.1% Pt/$SiO_2$ samples were prepared by the incipient wetness method, while an excess water technique was used to prepare the 1.5% Pt/$SiO_2$–$Al_2O_3$ (1.5% Pt/S-A) sample, and further details of both preparation methods are given elsewhere (*11*). One portion of the 2.1% Pt/$SiO_2$ sample was reimpregnated with pure water after initial preparation and drying overnight at 395 K, and is designated by a (W). The final platinum weight loadings of the catalysts were determined by neutron activation analysis using a known concentration of chloroplatinic acid in water as a standard.

### *Chemisorption Measurements*

*Apparatus.* The uptake measurements were made using one of two high-vacuum systems. The first consisted of a glass manifold connected to a 150-lpm Edwards Model E02 oil-diffusion pump backed by a mechanical pump with liquid-nitrogen traps at the inlet of each pump. An ultimate dynamic vacuum near $4 \times 10^{-7}$ Torr (1 Torr = 133 Pa) was obtainable, as measured by a Granville-Phillips Model 260-002 ionization gauge. Isotherm pressures and temperatures were measured by a Texas Instruments Model 145 precision gauge and a Doric digital trendicator, respectively. A more detailed description of the gases, their purification, and the adsorption system is given elsewhere (*11*). The second adsorption system was constructed of stainless steel, utilized an Edwards Diffstak MK2 oil diffusion pump, and provided an ultimate vacuum below $10^{-8}$ Torr. Isotherm pressures were again measured by a TI 145 gauge, but heating rates and temperature control were provided by a Theal Engineering programmer/controller. Details of this system are given elsewhere (*12*).

*Procedure and pretreatments.* Approximately 0.5 g of fresh catalyst was placed in a Pyrex adsorption cell, and each sample was given pretreatment A, B, or C, as listed in Table 1, prior to the adsorption runs. Pretreatment A was followed for Pt supported on $\eta$-$Al_2O_3$, $SiO_2$–$Al_2O_3$, and $SiO_2$, while both pretreatments B and C were used for Pt/$TiO_2$ (*1*). The low-temperature

TABLE 1

Pretreatment Procedures

| Pretreatment A[a] |
|---|
| 1. Heat sample to 393 K in flowing He (or Ar), and hold for 30 min |
| 2. Switch to flowing $H_2$ (or $H_2$/Ar), heat to 533 K, and hold in flowing $H_2$ for 30 min |
| 3. Heat to final temperature of 723 K and maintain for 1 h in flowing $H_2$ |
| 4. Cool to 698 K in flowing $H_2$, evacute (in adsorption system), or purge in Ar (in DSC system) at 698 K for 1 hr, then cool |
| **Pretreatment B[a] (LTR)** |
| 1. Heat sample to 423 K in flowing He (or Ar), and hold for 30 min |
| 2. Switch to flowing $H_2$ (or $H_2$/Ar), heat to 473 K, and hold in flowing $H_2$ for 2 h |
| 3. Terminate $H_2$ flow, evacuate at 473 K (or purge in Ar) for 2 h, then cool |
| **Pretreatment C[a] (HTR)** |
| 1. Heat sample to 423 K in flowing He (or Ar), and hold for 30 min |
| 2. Switch to flowing $H_2$ (or $H_2$/Ar), heat to 773 K, and hold in flowing $H_2$ for 1 h |
| 3. Cool to 723 K in flowing $H_2$, evacuate (in adsorption system), or purge in Ar (in DSC system) at 723 K for 30 min, then cool |

[a] All heating rates were 40 K/min.

reduction at 473 K (B) is designated (LTR), while the high-temperature reduction at 773 K (C) is designated (HTR). After initial pretreatment, the catalyst was cooled under dynamic vacuum to either 300 or 215 K prior to the adsorption run. For the low-temperature chemisorption experiments, the sample cell was placed in a Dewar flask containing a slurry of chloroform and dry ice.

The chemisorption of hydrogen on pure $\eta$-$Al_2O_3$, $SiO_2$–$Al_2O_3$, and $TiO_2$ has already been shown to be zero at room temperature (*11, 13*), and the $H_2$ uptake on $TiO_2$ (LTR) and $TiO_2$ (HTR) was found in this study to also be zero at 215 K. The isotherms for hydrogen at both ambient temperature and 215 K covered a pressure range of 50 to 400 Torr and were essentially linear in this range, so the method of Benson and Boudart (*14*) and Wilson and Hall (*15*) was used to measure saturation hydrogen coverages on the Pt by extrapolating the isotherm to zero pressure. Two hydrogen isotherms were measured for the supported Pt catalysts at 215 K since reversible adsorption was more significant at this temperature. After the initial isotherm the sample was evacuated for 5 min at 215 K to remove weakly bound $H_2$, and the second isotherm was determined. The difference between the two isotherms at 75 Torr was chosen to represent the irreversible adsorption of hydrogen on the platinum surface at 215 K in the calorimetric measurements.

*Calorimeteric Measurements*

Isothermal energy changes were measured using a modified Perkin–Elmer DSC-2C differential scanning calorimeter with an Intracooler II (Model 319-0207) to allow subambient runs down to 200 K. The gas-handling system preceding the calorimeter controlled the flows of argon, helium, hydrogen, and carbon monoxide and provided switching capability between gas streams, as shown in Fig. 1. Ultrahigh purity argon (99.999% from MG Scientific Gases) was further purified by passing it first through a drying tube containing 5A molecule sieve (Supelco Inc.), and then through an Oxy-trap (Alltech Associates) before use as a purge gas in the calorimeter. The helium (99.999% from MG Scientific) was purified in a similar fashion. An Elhygen Mark V Hydrogen Generator produced ultrapure hydrogen (less than 10 ppb total impurities) by electrolytically dissociating deionized water and then diffusing the hydrogen through a thin palladium membrane. The carbon monoxide (99.99% from Matheson) was passed through a molecular sieve trap held at 383 K to remove any metal carbonyls. The gases were regulated by Tylan mass flow controllers (Model FC260), and a digital Tylan R020A readout box provided

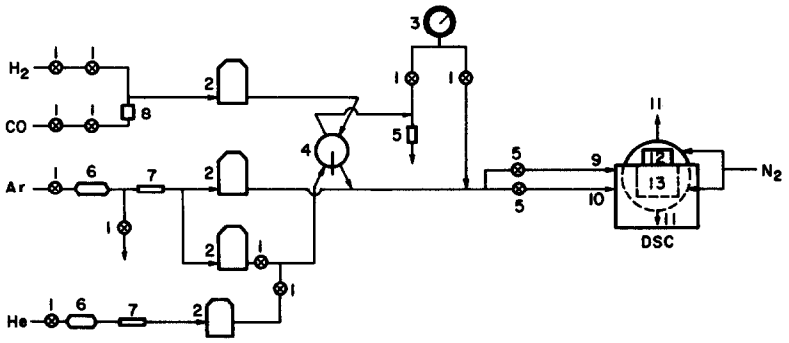


FIG. 1. Differential scanning calorimetry system: 1—Hoke valves, 2—mass flow controllers, 3—pressure gauge, 4—four-way switching valve, 5—needle valves, 6—Supelco drying tubes, 7—Oxy-traps, 8—molecular sieve trap, 9—line to sample cavity, 10—line to reference cavity, 11—$N_2$ purge streams through plastic shrouds, 12—draft shield, 13—aluminum block.

control and monitoring for the four mass flow controllers. Two of these controllers were capable of measuring between 0 and 50 $cm^3$ $min^{-1}$ argon flow, the third one was designed for either hydrogen or carbon monoxide flow control between 0 and 10 $cm^3$ $min^{-1}$, depending upon which valve was opened, and the fourth regulated He flows up to 10 $cm^3$ $min^{-1}$.

To enhance sensitivity and accuracy by minimizing baseline perturbations after switching from the purge gas to the gas stream containing the adsorbate, a number of evolutionary modifications were made to the gas-handling system and the calorimeter itself, and the final flow design is shown in Fig. 1. The changes to the DSC included: (1) perforation of the platinum sample holder covers to enhance gas mixing; (2) removal of the flow splitter inside the DSC and insertion of a needle valve in each line (to the sample side and to the reference side); (3) regulation of flows by mass flow controllers; (4) utilization of adjustable He/Ar ratios in the purge stream; and (5) enclosure of the entire aluminum block, the cover, and the draft shield under a blanket of flowing $N_2$ (99% from Linde) to eliminate the possibility of oxygen (air) diffusing through any tiny leaks to the sample.

To provide optimum performance, the following procedure was used. Needle valve 5 controlling gas flow to the atmosphere was adjusted so that equal pressure drops were attained through both loops of the switching valve. This eliminated a perturbation during switching due to a pressure differential. Adjustment of the two needle valves in lines 9 and 10 balanced the flows through the sample and reference cavities at a constant overall flow rate. The purge gas to the DSC was comprised of a constant Ar flow of ~36 $cm^3$/min which bypassed the switching valve plus an additional component which passed through the switching valve. For the experiments with $H_2$, switching occurred from 8 $cm^3$ $min^{-1}$ He to 4 $cm^3$ $min^{-1}$ $H_2$ back to the He. These He flow rates (STP) minimized baseline perturbation and offset due to differences between the thermal conductivity of the mixture and pure Ar, a problem which was more severe with the $H_2$ mixtures. After these modifications, very reproducible results with minimal baseline correction were obtained, as indicated in Fig. 2 by the base-case traces after switching with pure support on both the sample and the reference sides. This figure also shows a typical baseline variation when pure Ar was used as the purge gas, rather than the He/Ar mixture. As mentioned, the offset occurs because of the difference in thermal conductivity of the two streams.

The signal output from the DSC and its time integral were monitored on a two-pen integrating recorder (Linear Instruments Model 252A). The energy calibration was conducted using various weights of indium and different ordinate (mcal/s) ranges, chart speeds, and heating rates to determine a calibration constant of $K = 0.0442 \pm 0.0002$ s/count for the recorder integrator. As a check, another $K$ value was determined based on the weight of the chart paper under the curve. Both provided excellent correlations, so the former was used in most cases. Only when energy changes

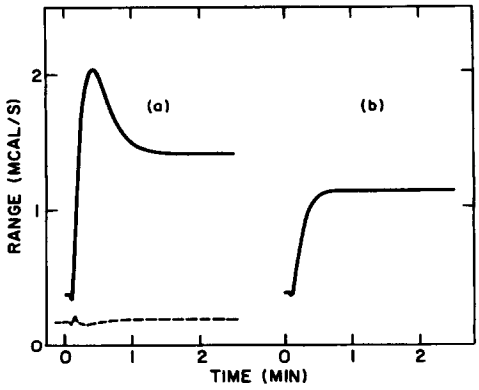


FIG. 2. Effect of carrier gas on baseline DSC curves for pure $TiO_2$. (a) Temperature at 320 K: solid line—switching from Ar to 10% $H_2$/90% Ar prior to insertion of needle valves. Dotted line: switching from 20% He/80% Ar to 10% $H_2$/90% Ar after installation of needle valves (optimum conditions). (b) Temperature at 215 K: switching from Ar to 10% $H_2$/90% Ar without needle valves.

were extremely small was the second procedure used. Eight ordinate sensitivities between 0.1 and 20 mcal $s^{-1}$ could be used, but with the sample sizes used here (0.03–0.15 g) and the typical gas uptakes that occurred, most runs could be easily recorded on a full-scale range of 2 or 5 mcal $s^{-1}$. After admittance of $H_2$ or CO, the baseline was corrected by subtracting the baseline trace of the pure support after exposure to that gas or by switching back to the purge gas for 3 min, reintroducing the adsorbate mixture, and obtaining the baseline trace after weakly adsorbed gas had been removed. On the "typical" catalysts using $Al_2O_3$, $SiO_2$, and $SiO_2$–$Al_2O_3$ the two traces were very similar; however, for the $TiO_2$ (HTR) samples some deviations occurred because of the small, more weakly adsorbed amounts of hydrogen occurring on the Pt. In these cases, the correction using the pure support was preferred.

The samples placed in the DSC were taken from larger (1–2 g) samples of that catalyst that had been previously pretreated and characterized in the chemisorption system then stored in a desiccator. Each sample was then given another pretreatment in the DSC in either a 10% $H_2$/90% Ar or a 20% $H_2$/80% Ar mixture, as noted, flowing at 40 $cm^3$ $min^{-1}$ and was heated at 40 K $min^{-1}$ to the desired temperature. Because of the greater thermal conductivity of $H_2$, significant deviations occurred between the actual cavity temperature and the temperature indicated on the DSC when pure $H_2$ was used. For example, with a flow of pure $H_2$, used in certain cases, a maximum temperature of 713 K was achieved rather than the indicated 773 K. A calibration between $\Delta T$ and the $H_2$ mole fraction allowed the actual temperature to be obtained.

Finally, to check for possible contamination effects, the purge time at high temperature in the DSC system was varied from 20 to 660 min as a $N_2$ blanket was kept around the cavity. The total energy change increased about 30% as purge time increased up to 60 min, which was attributed to an increase in desorption from the surface. Additional purging to 180 min produced no change, within experimental error, and a 660-min purge results in a 5% increase in the energy change. Consequently, 60 min was chosen as an optimum time for complete removal of hydrogen from the surface. As an additional test, a $Pt/TiO_2$ (HTR) sample was pretreated and purged, then cooled to 300 K, and left under flowing Ar overnight while the $N_2$ blanket was maintained. The measured energy change after this long-term exposure was 39.3 mcal/g compared to the previous value of 38.7 mcal/g obtained after our normal procedure. This deviation was within experimental error and again showed the absence of any contaminants entering with the Ar or via any air leaks.

## RESULTS

Saturation hydrogen uptakes at 300 K and both the total and irreversible hydrogen uptakes at 215 K are listed in Table 2 along with Pt dispersions (fractions exposed) and crystallite sizes calculated assuming equal areas of the (100), (110), and (111) crystal planes and using the equation $d_s$ (nm) = $1.13/D$ where $d_s$ is the surface-weighted diameter and $D$ is the fraction exposed, i.e., the H/Pt ratio (*8*).

Table 3 contains the calorimetric data including the number of runs made on a given sample to obtain the listed average energy change after baseline corrections. The standard deviations include errors inherent in both the chemisorption and the energy change measurements, and they represent maximum deviations because in actuality some of the systematic errors in the chemisorption procedure tend to cancel out. Figures 3 and 4 show sets of calorimetric data for 2.1% $Pt/\eta$-$Al_2O_3$ and 1.5% $Pt/TiO_2$ (LTR) which were obtained before the system was optimized. In these figures the baseline offset was due to the difference in thermal conductivity between a pure Ar purge and a 10% $H_2$/90% Ar stream, and

TABLE 2

$H_2$ Adsorption on Supported Pt

| Catalyst | Uptake ($\mu$mole g cat$^{-1}$) | | | Pt fraction exposed[a] (H/Pt) | Pt crystallite size (nm) |
|---|---|---|---|---|---|
| | 300 K | 215 K | | | |
| | | Irrev. | Total | | |
| 2.1% Pt/$\eta$-$Al_2O_3$ | 39.9 | 41.7 | 48.1 | 0.74 | 1.5 |
| 1.5% Pt/$SiO_2$–$Al_2O_3$ | 15.1 | — | — | 0.39 | 2.9 |
| Pure $TiO_2$ (LTR) | 0.0[b] | 0.0 | — | — | — |
| 1.5% Pt/$TiO_2$ | 38.5 | 25.5 | 30.6 | 1.00 | 1.1 |
| 2.0% Pt/$TiO_2$ | | | | | |
| I | 49.7 | | | 0.97 | |
| II | 31.5 | | | 0.61 | |
| II[c] | 31.8 | | | 0.62 | |
| IIA[d] | 23.0 | | | 0.45 | |
| Pure $TiO_2$ (HTR) | 0.0[b] | 0.0 | | | |
| 1.5% Pt/$TiO_2$ (HTR) | 1.5 | 1.9 | 2.6 | [0.039] | 1.1 |
| 2.0% Pt/$TiO_2$ (HTR) | | | | | |
| I | 1.0 | | | [0.020] | |
| II | 1.6 | | | [0.031] | |
| IIA[d] | 1.4 | | | [0.027] | |
| III | 1.0 | | | [0.020] | |
| 2.1% Pt/$SiO_2$ | | | | | |
| I | 4.1 | 6.6 | 8.6 | 0.076 | 14.8 |
| II | 15.2 | | | 0.28 | 4.0 |
| 2.1% Pt/$SiO_2$ (W) | | | | | |
| III | 9.1 | | | 0.17 | 6.7 |

[a] Based on adsorption at 300 K.
[b] Ref. (*13*).
[c] Average of four uptakes, rather than the first three included in II.
[d] A—after $O_2$ treatment (see Table 3).
(W)—Water-treated catalyst (see text).

the sizable peak immediately after switching was because of slightly unequal flow rates through each side. The improvement achieved after all modifications were completed is obvious in Figs. 5 and 6, which show another run for 2.0% Pt/$TiO_2$ (LTR) and a run for 2.1% Pt/$SiO_2$, both conducted under the more optimum conditions. In all cases, the energy change, $\Delta H$, in millicalories per gram is represented by the area between the two curves. The improvement in baseline was not especially important in samples which had large exotherms and results were reproducible under nonoptimum conditions; for example, compare the 2.1% Pt/$\eta$-$Al_2O_3$ catalyst—Sample I was before and Sample II was after optimization—and compare the 1.5% Pt/$TiO_2$ (LTR) catalyst (before) with the 2.0% Pt/$TiO_2$ (LTR) catalyst (Sample III) (after optimization).

As shown in Fig. 7, results for the Pt/$TiO_2$ (HTR) samples were the most difficult to obtain not only because the uptakes and energy changes decreased markedly, thus increasing the uncertainties of their measurements, but also because these low values were extremely dependent upon subtleties in the pretreatment procedure and the number of pretreatment cycles. Consequently we found that to obtain consistent, reproducible results it was *imperative* that samples be given *identical* pretreatments in the chemisorption unit and the DSC, that

TABLE 3

Heats of Adsorption of Hydrogen on Supported Platinum

| Catalyst | Sample | Weight (mg) | Pretreatment | Adsorption temperature (°K) | No. of runs | Average energy change, $\Delta H$ (mcal/g) | $\Delta H_{(ad)}$ (kcal/mole) [a] | $\Delta H_{(ad)}$ (kcal/mole) [b] |
|---|---|---|---|---|---|---|---|---|
| 2.1% $Pt/\eta$–$Al_2O_3$ | | | | | | | | |
| | I | 60.6 | A | 320 | 2 | 1109 | — | 27.8 ± 1.1 |
| | | | A | 215 | 4 | 617 | 14.8 ± 0.5 | 12.8 ± 0.4 |
| | II | 62.7 | A | 320 | 3 | 1003 | — | 25.1 ± 0.7 |
| | | | A | 215 | 4 | 601 | 14.4 ± 0.5 | 12.5 ± 0.4 |
| 1.5% $Pt/SiO_2$–$Al_2O_3$ | | | | | | | | |
| | I | 32.3 | A | 320 | 2 | 439 | — | 29.1 ± 1.9 |
| | II | 34.5 | A | 320 | 4 | 415 | — | 27.5 ± 2.5 |
| 2.1% $Pt/SiO_2$ | | | | | | | | |
| | I | 33.7 | A | 320 | 2 | 148 | — | 36.1 ± 6.9 |
| | | | A | 215 | 2 | 48 | 7.4 ± 1.7 | 5.7 ± 1.2 |
| 2.1% $Pt/SiO_2$ | | | | | | | | |
| | II | 36.9 | A | 300 | 3 | 421 | — | 27.7 ± 3.0 |
| 2.1% $Pt/SiO_2$(W) | | | | | | | | |
| | III | 37.3 | A | 320 | 5 | 313 | — | 34.4 ± 4.7 |
| 1.5% $Pt/TiO_2$ (LTR) | | | | | | | | |
| | I | 40.6 | B | 320 | 3 | 807 | — | 21.0 ± 0.7 |
| | | | B | 215 | 3 | 373 | 14.6 ± 0.6 | 12.2 ± 0.5 |
| 2.0% $Pt/TiO_2$ (LTR) | | | | | | | | |
| | I | 99.5 | B | 300 | 3 | 818 | — | 25.7 ± 0.9 |
| | II | 98.4 | B | 300 | 4 | 854 | — | 27.1 ± 2.3 |
| | IIA[c] | 98.4 | B | 300 | 4 | 524.4 | — | 22.8 ± 3.1 |
| | III | 91.8 | B | 300 | 2 | 1049.6 | — | 21.1 ± 0.5 |
| | IV | 106.2 | B | 300 | 4 | 868.0 | — | 27.6 ± 3.6 |
| | IVA[c] | 106.2 | B | 300 | 4 | 595.5 | — | 25.9 ± 3.7 |
| 1.5% $Pt/TiO_2$ (HTR) | | | | | | | | |
| | I | 41.4 | C | 320 | 1 | 8.5 | — | 5.7 |
| | II | 64.5 | C | 320 | 3 | 4.5 | — | 3.0 ± 2.0 |
| 2.0% $Pt/TiO_2$ (HTR) | | | | | | | | |
| | I | 108.6 | C | 300 | 4 | 13.8 | — | 13.8 ± 12.2 |
| | II | 98.4 | C | 300 | 3 | 16.6 | — | 10.4 ± 10.5 |
| | IIA[c] | 98.4 | C | 300 | 3 | 13.9 | — | 9.9 ± 4.4 |
| | IV | 106.2 | C | 300 | 3 | 16.4 | — | 10.3 ± 5.2 |
| | IVA[c] | 106.2 | C | 300 | 4 | 27.4 | — | 19.4 ± 8.1 |

[a] Based on irreversible adsorption on Pt.
[b] Based on total adsorption on Pt.
[c] A indicates values obtained after treatment in 20% $O_2$/80% He at 673 K for 30 min followed by an LTR or HTR step, as listed in the table.

chemisorption measurements be made after every pretreatment cycle, and that the order and number of pretreatment cycles be kept identical in the DSC and adsorption systems. A typical sequence of experiments for a $Pt/TiO_2$ sample and the corresponding data obtained after each pretreatment step are listed in Table 4.

## DISCUSSION

The heat of adsorption of hydrogen on Pt surfaces has been determined in many studies which have employed a variety of techniques such as thermal desorption, calorimetry, work function measurements, adsorption isosteres, field emission microscopy, and theoretical calculations. The results from these earlier studies are tabulated in the review by Toyashima and Somorjai (*16*) and in the paper by Cerny *et al.* (*17*). A wide range of $\Delta H_{ad}$ values from below 10 to over 50 kcal/mole has been reported; however, if only the more recent results obtained in UHV systems are considered, the variation in $\Delta H_{ad}$ near 300 K is substantially decreased and values range between 12 and 32 kcal/mole, with most falling between 20 and 30 kcal/mole. Still, on the Pt(111) plane alone, reported values vary from ~17 to ~31 kcal/mole (*16*). Studies of supported Pt are far less numerous,

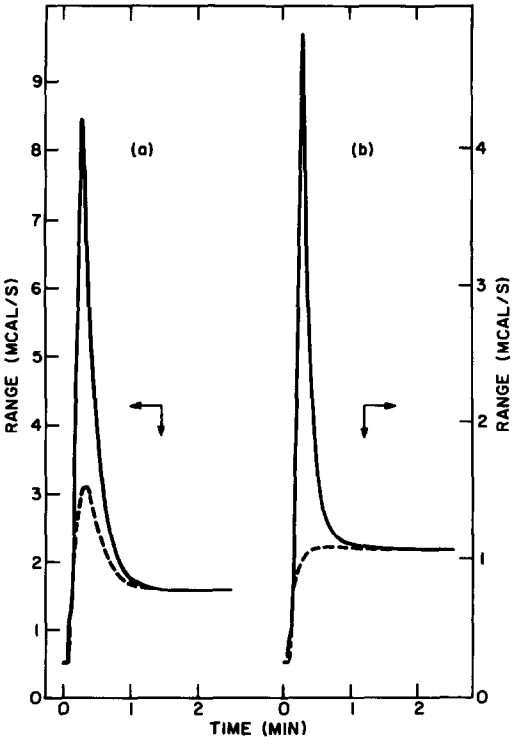


FIG. 3. DSC curves for $H_2$ adsorption on 2.1% Pt/$\eta$-$Al_2O_3$ prior to optimized conditions (60.6 mg). Dotted lines represent baselines obtained during readsorption following a 3-min purge: (a) 320 K, (b) 215 K.

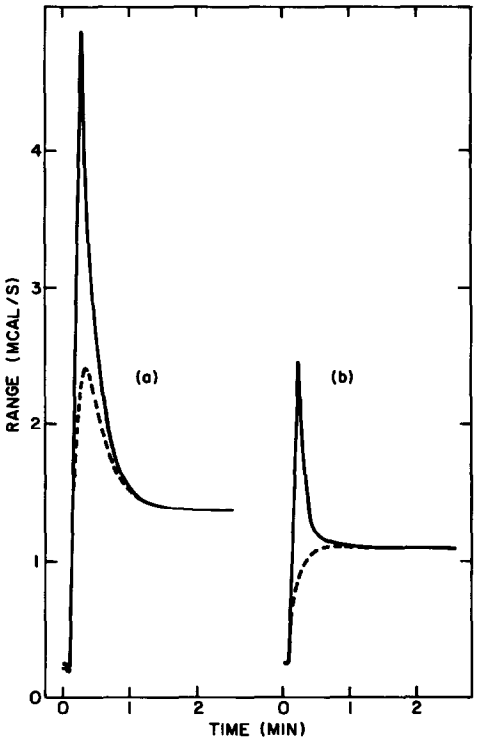


FIG. 4. DSC curves for $H_2$ adsorption on 1.5% Pt/$TiO_2$ (LTR) prior to optimized conditions (40.6 mg). Dotted lines represent baselines obtained during readsorption after a 3-min purge: (a) 320 K, (b) 215 K.

TABLE 4

Effect of Pretreatment Cycles on $H_2$ Uptake and Heat of Adsorption for $TiO_2$-Supported Pt

| Sample II (98.4 mg 2.0% Pt/$TiO_2$ in DSC) | | | | |
|---|---|---|---|---|
| Run sequence | Pretreatment | Energy change (mcal/g cat) | Uptake ($\mu$mole/g cat) | $\Delta H_{(ad)}$ (kcal/mole) |
| 1 | B (LTR) | 939.6 | 32.9 | 28.6 |
| 2 | B | 889.4 | 31.6 | 28.1 |
| 3 | B | 815.3 | 30.8 | 26.5 |
| 4 | B | 772.6 | 30.7 | 25.2 |
| 5 | C (HTR) | 34.0 | 2.0 | 17.0 |
| 6 | C | 10.0 | 1.4 | 7.1 |
| 7 | C | 5.8 | 1.3 | 4.5 |
| 8[a] | B (LTR) | 606.4 | 21.9 | 27.7 |
| 9 | B | 561.5 | 22.7 | 24.7 |
| 10 | B | 468.1 | 23.4 | 20.0 |
| 11 | B | 461.8 | 24.0 | 19.2 |
| 12 | C (HTR) | 14.4 | 1.1 | 13.1 |
| 13 | C | 15.3 | 1.8 | 8.5 |
| 14 | C | 12.1 | 1.3 | 9.3 |

[a] Catalyst treated in 20% $O_2$ + 80% Ar(He) at 400°C for 30 min between Runs 7 and 8.

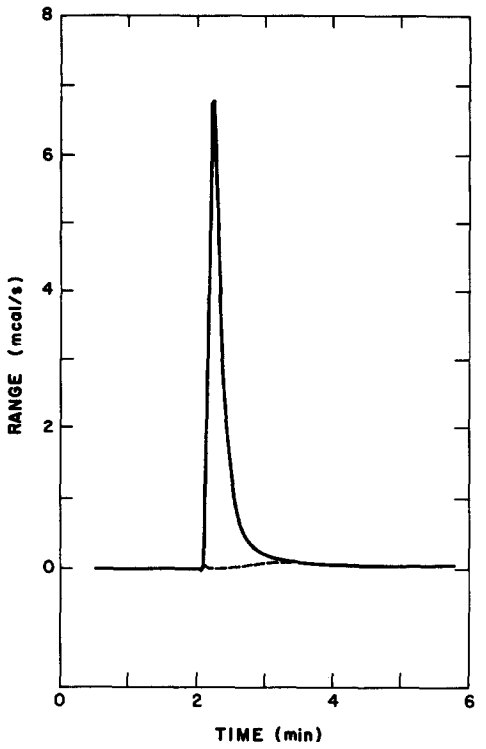


FIG. 5. DSC curve for $H_2$ adsorption at 300 K on 2.0% $Pt/TiO_2$ (LTR) after optimization (106.2 mg). Dotted line represents baseline obtained from pure $TiO_2$.

and only three studies since 1970 have appeared in the literature (*18–20*); regardless, a similar variation exists and $\Delta H_{ad}$ ranges from 10 to 36 kcal/mole. Obviously, the possibility of contamination is a major concern in the older studies, particularly those involving Pt black because of the concentration of residual impurities at the surface (*21*).

The values listed in Table 3 represent isothermal, integral heats of adsorption corresponding to the total energy change that occurs as an initially clean Pt surface reaches adsorption equilibrium under 75 Torr $H_2$. The direct calorimetric measurement of heats of adsorption has certain advantages over isosteric and TPD techniques. For example, diffusional and readsorption effects have no influence upon these values. Also, any irreversible adsorption renders use of the Clausius–Clapeyron equation unreliable and values obtained by this method are typically low. A reasonably wide spread of heats of adsorption exists among the catalysts which might be expected to exhibit normal adsorption behavior, yet these $\Delta H_{ad}$ values near 300 K readily fall within the range previously reported and all but two lie between 20 and 30 kcal/mole. Perhaps the most surprising results are the relatively high values near 35 kcal/mole for two of the $Pt/SiO_2$ samples. We had anticipated that our integral $\Delta H_{(ad)}$ values would be noticeably lower than the initial desorption energies ($E_d \geq \Delta H_{(ad)}$) acquired from TPD runs. The result that they are comparable may be a consequence of intrinsic limitations in TPD studies due to appropriate choice of the frequency factor and the order of the desorption process, both of which affect the $E_d$ value. Another explanation may be that our use of higher $H_2$ pressures enhances the filling of high-energy binding states on these Pt crystallites which have an

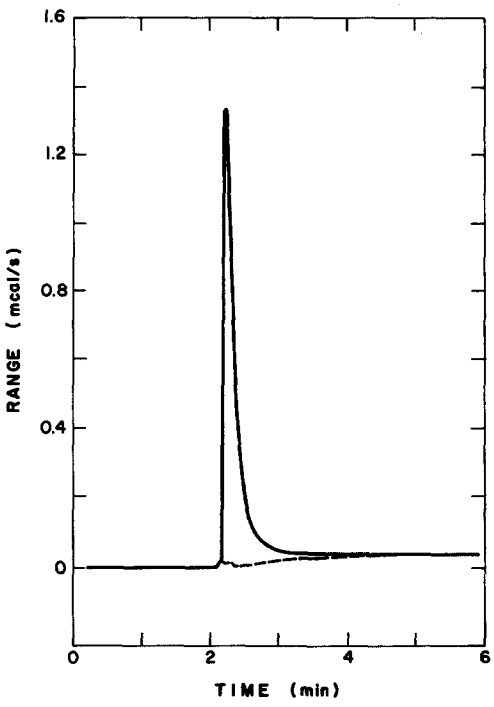


FIG. 6. DSC curve for $H_2$ adsorption at 300 K on 2.1% $Pt/SiO_2$ after optimization (36.9 mg). Baseline was obtained from pure $SiO_2$.

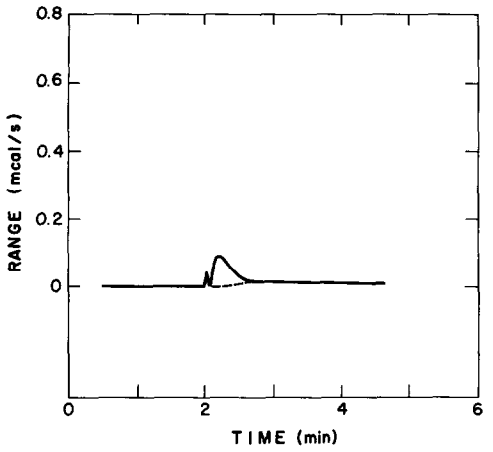


FIG. 7. DSC curve for adsorption at 300 K on 2.0% $Pt/TiO_2$ (HTR) (106.2 mg). Baseline was obtained from pure $TiO_2$.

activation barrier and are not filled (or do not exist) on low-index single crystals. A third possibility is that certain crystallite geometries may be favored in these supported catalysts, such as square (cubic) Pt particles which can be formed on $SiO_2$ (*22*). The fraction of the surface comprised of the (100) plane, which has fourfold symmetry, might be markedly higher than usual, and McCabe and Schmidt have reported the highest $E_d$ values (27.5 kcal/mole) for this plane (*23*). As mentioned under Experimental, we cannot attribute these somewhat higher $\Delta H_{(ad)}$ to contamination effects and, because the highest values were achieved using $SiO_2$, typically assumed to be an inert, noninteracting support, we do not believe it is due to a metal–support interaction.

Although support effects upon adsorption bond strength must be considered in this group of catalysts, which includes $Pt/TiO_2$ after a LTR step, crystallite size may be an equally important parameter, as indicated by Fig. 8. If the support is not considered, a clear trend appears to exist between $\Delta H_{ad}$ and Pt dispersion, as represented by the H/Pt ratios, with bond strength decreasing along with crystallite size in a uniform manner. This trend is opposite to that expected if stronger bonding is associated with Pt atoms of lower coordination number such as edge and corner sites (*24, 25*). However, the study of McCabe and Schmidt found the highest binding energies on the (100) plane, followed by the more open (210) and (211) surfaces, then the (111) plane, and finally the (110) surface, which had the lowest values (*23*). An average integral $\Delta H_{(ad)}$ value was determined from the data of Lantz and Gonzalez (*20*), and it is also represented in Fig. 8. Although it appears somewhat low compared to our values, it is consistent with the observed trend. We are now preparing a range of Pt dispersions on $SiO_2$ to determine if this apparent crystallite size effect does indeed exist.

Some initial results measuring heats of adsorption at 215 K are also contained in Table 3. In all cases $\Delta H_{(ad)}$ values are significantly lower, which is consistent with TPD studies showing that additional lower-energy binding states are filled at lower temperatures (*23, 26*). Hydrogen uptakes were

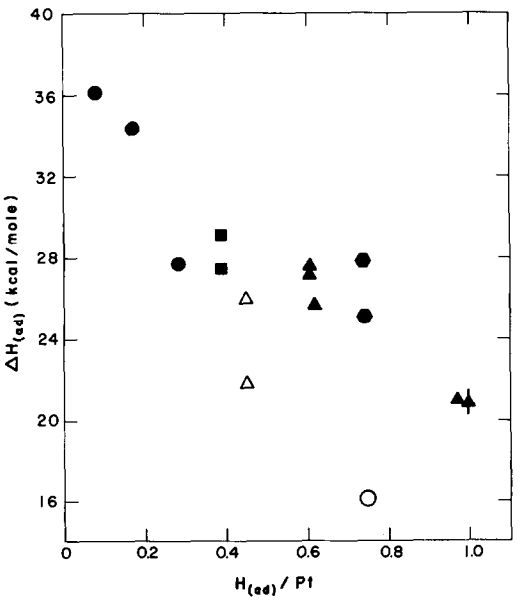


FIG. 8. Correlation of $H_2$ heat of adsorption with Pt dispersion: 2.1% $Pt/SiO_2$ (●), 1.5% $Pt/SiO_2$–$Al_2O_3$ (■), 2.1% $Pt/\eta$-$Al_2O_3$ (●), 2.0% $Pt/TiO_2$ (LTR) (▲), 2.0% $Pt/TiO_2$ (LTR) after $O_2$ exposure and rereduction (△), 1.5% $Pt/TiO_2$ (LTR) (▲), $Pt/SiO_2$ [from Ref. (*20*)] (○).

higher at 215 than at 300 K for all catalysts studied except the LTR 1.5% $Pt/TiO_2$ sample. This trend is expected for nonactivated adsorption and the behavior of the LTR $Pt/TiO_2$ may indicate the presence of a small activation barrier presumably introduced by the presence of the titania. The $\Delta H_{(ad)}$ values for the $Pt/Al_2O_3$ and LTR $Pt/TiO_2$ correspond more closely with the $\beta_2$ and $\beta_3$ desorption states on the (110) and (100) planes and the $\beta_1$ state on the (211) surface while the heat of adsorption on the $Pt/SiO_2$ sample agrees most closely to the $\beta_1$ state on the (100) plane (*23*). This again suggests that the latter plane predominates on the Pt crystallites in this catalyst. Although the HTR $Pt/TiO_2$ catalyst exhibited a small increase in uptake at 215 K, no measurable exotherm was detected in the calorimeter. This suggests a modification of the few remaining adsorption sites which results in adsorption only in weakly bonding states that can be populated at lower temperature.

The results obtained for $Pt/TiO_2$ after an HTR clearly do not fit the trend found with the "typical" catalysts. Previously, studies on $Pt/TiO_2$ catalysts by Baker *et al.* have shown that Pt crystallite size changes little during this treatment (*27, 28*), and dispersions cannot increase further as they are unity for our most well-dispersed $Pt/TiO_2$ samples. No evidence has been reported to show that "atomic" dispersion, i.e., single isolated Pt atoms, exists in these $Pt/TiO_2$ systems and, in fact, the formation of Pt rafts has been proposed (*27, 28*). Consequently, we conclude that some change which weakens the H–Pt bond, not associated with crystallite size per se, has occurred at the Pt surface after an HTR step. This decrease in $\Delta H_{(ad)}$ is responsible, at least partially, for the reduced $H_2$ chemisorption capacity of "SMSI" $Pt/TiO_2$ systems (*1, 2*). We interpret these results to be direct calorimetric verification that metal–support interactions in $TiO_2$-supported Pt decrease the adsorbate bond strength. However, this behavior cannot be generalized to all Group VIII metals because similar results were not observed for $Pd/TiO_2$ catalysts (*29*). Our results for $Pt/TiO_2$ (HTR) are consistent with the recent study of White and co-workers who found that $H_2$ desorbed at lower temperatures from Pt deposited on reduced $TiO_2$, compared to Pt on oxidized $TiO_2$ (*30*). Our results are also similar to those in the TPD study of Weatherbee and Bartholomew which showed that adsorbed hydrogen was shifted to lower-energy binding states in $Ni/TiO_2$ catalysts (*31*). However, in a similar study on Ni foils under UHV conditions, Raupp and Dumesic did not observe this effect when $TiO_x$ was placed on a Ni surface, and two additional higher-energy binding states were created in addition to a lower-energy state, compared to clean Ni (*32*).

The data in Tables 3 and 4 show that the "SMSI" behavior can be reversed by exposure to oxygen at higher temperatures, as reported in the literature (*1, 2, 27, 28*). However, the significant influence of pretreatment time and temperature is indicated in Table 4, which shows a series of concomitant runs in the DSC and adsorption systems on a single sample of $Pt/TiO_2$. Successive LTR cycles slowly decreased both $H_2$ uptakes and $\Delta H_{(ad)}$ values, but the surface appeared to stabilize after about four successive cycles. This is assumed to be a result of the surface reduction of $TiO_2$ and slow migration of $TiO_x$ species onto the Pt, which can occur to some extent even at 473 K. The effect of HTR cycles is much more pronounced, and although chemisorption is markedly decreased after only one cycle, the greatest decrease in $\Delta H_{(ad)}$ values seems to occur after the second and third cycles. The variation in uptakes after the HTR steps is small on an absolute basis but large on a relative basis, hence the heats of adsorption are very sensitive to these measurements. We readily admit that the sensitivities of both systems were being tested in these experiments and it is gratifying that the low $\Delta H_{(ad)}$ values obtained could be reproduced as well as they were. Table 4 substantiates our warning that the surface of

these $Pt/TiO_2$ systems is extremely sensitive to experimental parameters such as time and temperature of reduction, $H_2$ pressure, and the number of reduction cycles; therefore, great care must be taken in obtaining results with similar "SMSI" catalysts. This sensitivity to pretreatment conditions could readily account for the differences in behavior reported for $Ni/TiO_2$ systems (*31, 32*).

Much evidence has been obtained recently which shows that in metal/$TiO_2$ systems a titanium oxide species ($TiO_x$) can migrate onto the metal surface (*5–7, 33–38*). As a result, we attribute much of the decrease in chemisorption on $TiO_2$-supported Pt, and "SMSI" catalysts in general, to physical blockage of Pt surface sites due to migration of $TiO_x$ species during the HTR step. The remaining adsorption sites, however, are modified and exhibit lower average bond strengths as shown by our measurements. Activated adsorption may also be enhanced in these $Pt/TiO_2$ systems. These adsorption sites may still be associated with Pt atoms only, or they may represent newly created sites at the Pt–$TiO_x$ interface (*39–42*), or they may be situated on the $TiO_2$ surface away from the interface region—evidence exists for all three possibilities (*7, 41–45*). We believe our measurements have principally detected the first two types of sites because of the low temperatures used, which would slow surface diffusion, and previous IR studies of CO absorbed on $Pt/TiO_2$ which showed bands associated only with Pt–CO bonds (*46*). The calorimetric results reported here, therefore, are strong evidence that the electronic nature of these surface Pt atoms has been significantly altered due to electron transfer resulting from either: (1) localized Pt–$TiO_x$ bonding (*2*); (2) metal–semiconductor behavior dependent upon the bulk properties of the support (*5, 47, 48*); or (3) a promotor effect (*4, 7*). However, changes in Pt morphology cannot be ruled out. Although we cannot distinguish among these possibilities, a change in the chemical nature of surface Pt atoms because of its contact with a $TiO_x$ surface is clearly indicated.

The specific activities for methanation over these catalysts have been measured, and turnover frequencies vary more than 100-fold (*8*). There is a correlation between $CH_4$ turnover frequency and $\Delta H_{(ad)}$, as shown in Fig. 9. It is nearly identical to that found between $N_{CH_4}$ and $\Delta H_{(ad)}$ for CO (*10*). Although a previously proposed kinetic model for methanation would predict that a decrease in $\Delta H_{(ad)}$ for $H_2$ would result in a higher apparent activation energy, a larger preexponential factor, and a rate enhancement (*8*), all of which is observed, we do not think that this in itself is a completely adequate explanation. We prefer the proposal that active sites are created at the Pt–support interface which have an enhanced

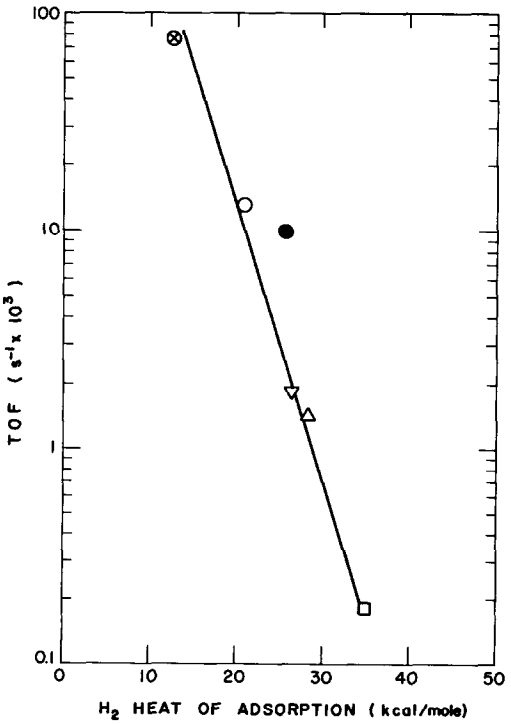


FIG. 9. Correlation of $CH_4$ turnover frequency with $H_2$ heat of adsorption on supported platinum: 2.1% $Pt/SiO_2$ (□), 1.5% $Pt/SiO_2$–$Al_2O_3$ (△), 2.1% $Pt/\eta$-$Al_2O_3$ (▽), $Pt/TiO_2$ (LTR) (high dispersion) (○), $Pt/TiO_2$ (LTR) (average of all samples) (●), $Pt/TiO_2$ (HTR) (average of all samples) (⊗).

capability to rupture the CO bond when certain supports are utilized, and these new sites provide the higher activity because this is the slow step on Pt (*8, 40*). Intuitively, it is difficult to associate very weak hydrogen adsorption with higher activity, and we suggest that the correlation may not represent a cause and effect situation. That is, some alteration of the Pt surface occurs which simultaneously creates new active sites and decreases the *average* heat of adsorption on the available Pt atoms, all of which need not be active sites. In fact, evidence indicates that only a small fraction of surface Pt atoms constitute "active sites" (*8*). Consequently the variation in hydrogen heats of adsorption, representing the entire Pt surface, is not the direct cause for the higher activity.

Experiments are currently in progress to test this hypothesis. The different Pt crystallite sizes on a given support which will be studied by calorimetry will also be characterized by kinetic studies to determine if a marked variation in $\Delta H_{(ad)}$, should it occur, correlates with activity as it does in Fig. 9. As no Pt crystallite size effect on $CH_4$ turnover frequency exists when a given support is used (*8*), this would help distinguish between the effect of adsorption parameters on rates versus the creation of special interface sites.

## SUMMARY

In this study, we have measured $H_2$ heats of adsorption on supported Pt under identical adsorption conditions using a sensitive, modified differential calorimeter. This allowed us to evaluate the influence of the support and of Pt crystallite size on isothermal, integral $\Delta H_{(ad)}$ values for Pt dispersed on $SiO_2$, $\eta$-$Al_2O_3$, $SiO_2$–$Al_2O_3$, and $TiO_2$. Heats of adsorption at 300–320 K ranged from 36 to 21 kcal/mole, and were highest on the $Pt/SiO_2$ samples and lowest on the (LTR) $Pt/TiO_2$ samples. This variation appears to be dependent upon both the support and crystallite size because a trend exists between $\Delta H_{(ad)}$ and dispersion irrespective of the support, with large Pt crystallites having the highest heats of adsorption. An HTR cycle induces dramatic decreases in both chemisorption and heat of adsorption, and the latter property can decline after repeated cycles to values near 5–10 kcal/mole at 300 K. This provides direct evidence that a decrease in the H–Pt bond strength is at least partially responsible for the lower chemisorption capacity. However, migration of the $TiO_x$ species onto the Pt under HTR conditions is assumed to cause physical blockage of some surface Pt sites as well as modification of the few remaining adsorption sites. A correlation exists between the $CH_4$ turnover frequency and the heat of adsorption for $H_2$, with the least active catalysts, $Pt/SiO_2$, having the highest heats of adsorption. This decreased surface bond strength, coupled with a concomitant decrease in CO heat of adsorption (*10*), could account for the observed increase in activity over $Pt/TiO_2$ catalysts; however, current evidence favors a model proposing that special Pt–$TiO_x$ interface sites enhance the CO hydrogenation reaction by facilitating C–O bond rupture (*39, 40*). Consequently, we do not view the correlation between $N_{CH_4}$ and $\Delta H_{(ad)}$ as a cause and effect relationship, but that of two parameters independently varying as changes occur in the chemical state of surface Pt atoms. Although these results show a decrease occurs in the H–Pt bond strength after HTR cycles, they cannot be generalized to include all the Group VIII, or even all the noble, metals because such behavior was not observed with $Pd/TiO_2$ catalysts and $H_2$ heats of adsorption were essentially independent of the support (*29*).

## ACKNOWLEDGMENTS

Support for this study came from the U.S. DOE, Division of Basic Energy Sciences, under Contract DE-AC02-77ERO 4463. We would also like to thank P. Chou for providing some of the DSC data.

## REFERENCES

*1.* Tauster, S. J., Fung, S. C., and Garten, R. L., *J. Amer. Chem. Soc.* **100,** 170 (1978).

2. Tauster, S. J., Fung, S. C., Baker, R. T. K., and Horsley, J. A., *Science* **211,** 1121 (1981).
3. Santos, J., Phillips, J., and Dumesic, J. A., *J. Catal.* **81,** 147 (1983).
4. Sachtler, W. M. H., *in* "Proceedings, 8th International Congress on Catalysis," I-151. Dechema, Frankfurt am Main, 1984.
5. (a) Meriadeau, P., Dutel, J., Dufaux, M., and Naccache, C., "Studies in Surface Science and Catalysis" (B. Imelik *et al.*, Eds.), Vol. 11. Elsevier, New York 1982; (b) Meriaudeau, P., Ellestad, O. H., Dufaux, N., and Naccache, C., *J. Catal.* **75,** 243 (1982).
6. Resasco, D. E., and Haller, G. L., *J. Catal.* **82,** 279 (1983).
7. Jiang, X.-Z., Hayden, T. F., and Dumesic, J. A., *J. Catal.* **83,** 168 (1983).
8. Vannice, M. A., and Twu, C.-C., *J. Catal.* **82,** 213 (1983).
9. Vannice, M. A., *J. Catal.* **50,** 228 (1977).
10. Vannice, M. A., Hasselbring, L. C., and Sen, B., *J. Catal.*, submitted.
11. Palmer, M. B., and Vannice, M. A., *J. Chem. Technol. Biotechnol.* **30,** 205 (1980).
12. Seyedmonir, S. R., Strohmayer, D. E., Geoffroy, G. L., and Vannice, M. A., *Adsorpt. Sci. Technol.*, in press.
13. Smith, J. S., Thrower, P. A., and Vannice, M. A., *J. Catal.* **68,** 270 (1981).
14. Benson, J. E., and Boudart, M., *J. Catal.* **4,** 704 (1965).
15. Wilson, G. R., and Hall, W. K., *J. Catal.* **17,** 190 (1970).
16. Toyashima, I., and Somorjai, G. A., *Catal. Rev.-Sci. Eng.* **19,** 105, (1979).
17. Cerny, S., Smutek, M., and Buzek, F., *J. Catal.* **38,** 245 (1975).
18. Basset, J. M., Theolier, A., Primet, M., and Prettre, M., *in* "Proceedings, 5th International Congress on Catalysis, Palm Beach, 1972" (J. W. Hightower, Ed.), pp. 63–915. North-Holland, Amsterdam, 1973.
19. Gentsch, H., Guillen, N., and Kopp, M., *Z. Phys. Chem.* **82,** 49 (1972).
20. Lantz, J. B., and Gonzalez, R. D., *J. Catal.* **41,** 293 (1976).
21. O'Rear, D., Ph.D. thesis. Stanford University, 1976.
22. Wang, T., Lee, C., and Schmidt, L. D., AIChE Annual Meeting, paper 127(a), San Francisco, Nov. 1984.
23. McCabe, R. W., and Schmidt, L. D., *in* "Proceedings, 7th Inst. Vac. Cong.," p. 1201. Vienna, 1977.
24. Taylor, H. S., *J. Phys. Chem.* **30,** 145 (1926).
25. Van Hardeveld, R., and Hartog, F., *in* "Advances in Catalysis" (D. E. Eley *et al.*, Eds.), Vol. 22, p. 75. Academic Press, New York, 1972.
26. McCabe, R. W., and Schmidt, L. D., *Surf. Sci.* **65,** 189 (1977).
27. Baker, R. T. K., Prestridge, E. B., and Garten, R. L., *J. Catal.* **56,** 390 (1979).
28. Baker, R. T. K., Prestridge, E. B., and Garten, R. L., *J. Catal.* **59,** 293 (1979).
29. Vannice, M. A., and Chou, P., *J. Chem. Soc. Chem. Commun.* 1590 (1984).
30. Belton, D. N., Sun, Y.-M., and White, J. M., *J. Phys. Chem.* **88,** 1690 (1984).
31. Weatherbee, G. D., and Bartholomew, C. H., *J. Catal.* **87,** 55 (1984).
32. Raupp, G. B., and Dumesic, J. A., *J. Phys. Chem.* **88,** 660 (1984).
33. Baker, R. T. K., Prestridge, E. B., and Murrell, L. L., *J. Catal.* **79,** 348 (1983).
34. Cairns, J. A., Baglin, J. E. E., Clark, G. J., and Ziegler, J. R., *J. Catal.* **83,** 301 (1983).
35. Sadeghi, H. R., and Henrich, V. E., *J. Catal.* **87,** 279 (1984).
36. Belton, D. N., Sun, Y.-M., and White J. M., *J. Phys. Chem.* **88,** 5172 (1984).
37. Taketani, S., and Chung, Y.-W., *J. Catal.* **90,** 75 (1984).
38. Ko, C. S., and Gorte, R. J., *J. Catal.* **90,** 59 (1984).
39. Burch, R., and Flambard, A. R., *J. Catal.* **78,** 389 (1982).
40. Vannice, M. A., and Sudhakar, C., *J. Phys. Chem.* **88,** 2429 (1984).
41. Beck, D. D., and White, J. M., *J. Phys. Chem.* **88,** 2764 (1984).
42. Beck, D. D., Bawagan, A. O., and White, J. M., *J. Phys. Chem.* **88,** 2771 (1984).
43. Huizinga, T., and Prins, R., *J. Phys. Chem.* **85,** 2156 (1981).
44. Apple, T. M., and Dybowski, C., *Surf. Sci.* **121,** 243 (1982).
45. Conesa, J. C., and Soria, J., *J. Phys. Chem.* **86,** 1392 (1983).
46. Vannice, M. A., Twu, C. C., and Moon, S. H., *J. Catal.* **79,** 70 (1983).
47. Herrmann, J. M., and Pichat, P., *J. Catal.* **78,** 425 (1982).
48. Chen, B.-H., and White, J. M., *J. Phys. Chem.* **86,** 3534 (1982).